Review

OPEN

The Utility of Spatial Transcriptomics for Solid Organ Transplantation

Jennifer S.Y. Li, MBBS, FRACP,[1,2] Arti M. Raghubar, MMolBiol,[3,4,5,6,7] Nicholas A. Matigian, MPhil,[8] Monica S.Y. Ng, MBBS, PhD,[3,4,6,7,9] Natasha M. Rogers, MBBS, FRACP, PhD,[1,2,10] and Andrew J. Mallett, MBBS, FRACP, PhD[6,7,11,12]

Abstract. Spatial transcriptomics (ST) measures and maps transcripts within intact tissue sections, allowing the visualization of gene activity within the spatial organization of complex biological systems. This review outlines advances in genomic sequencing technologies focusing on in situ sequencing–based ST, including applications in transplant and relevant non-transplant settings. We describe the experimental and analytical pipelines that underpin the current generation of spatial technologies. This context is important for understanding the potential role ST may play in expanding our knowledge, including in organ transplantation, and the important caveats/limitations when interpreting the vast data output generated by such methodological platforms.

(*Transplantation* 2023;107: 1463–1471).

INTRODUCTION

The field of solid organ transplantation is built on the combined pioneering endeavors of clinicians and researchers. These efforts have overcome, or at least moderated, many of the barriers to successful human transplantation, including improvements in surgical techniques and organ preservation methods, as well progressive understanding of transplant immunology, facilitating development of antirejection medications. However, over the past 2 decades, no new immunosuppressive medications have been approved by the Food and Drug Administration, stagnating progress that could improve graft and patient outcomes and contributing to unmet needs in solid organ transplantation.[1] The explosion of "Omics" technology

Received 20 June 2022. Revision received 19 October 2022.

Accepted 30 October 2022.

[1] Centre for Transplant and Renal Research, Westmead Institute for Medical Research, Westmead, NSW, Australia.

[2] Sydney Medical School, University of Sydney, Sydney, NSW, Australia.

[3] Kidney Health Service, Royal Brisbane and Women's Hospital, QLD, Australia.

[4] Conjoint Internal Medicine Laboratory, Pathology Queensland, Health Support Queensland, QLD, Australia.

[5] Department of Anatomical Pathology, Pathology Queensland, Health Support Queensland, QLD, Australia.

[6] Faculty of Medicine, University of Queensland, QLD, Australia.

[7] Institute for Molecular Bioscience, University of Queensland, QLD, Australia.

[8] QCIF Facility for Advanced Bioinformatics, The University of Queensland, QLD, Australia.

[9] Nephrology Department, Princess Alexandra Hospital, QLD, Australia.

[10] Department of Renal Medicine, Westmead Hospital, Westmead, NSW, Australia.

[11] College of Medicine and Dentistry, James Cook University, QLD, Australia.

[12] Department of Renal Medicine, Townsville University Hospital, QLD, Australia.

J.S.Y.L. and A.M.R. are joint first authors.

The authors declare that the research was conducted in the absence of any commercial or financial relationships that could be construed as a potential conflict of interest.

J.S.Y.L. is a recipient of the National Health and Medical Research Council (NHMRC) postgraduate scholarship (GNT116877) and the Westmead Association BJ Amos Travelling scholarship. A.M.R is a recipient of the Australian Government Research Training Program Scholarship and Pathology Queensland Research Committee fund. M.S.Y.N is supported by a Robert and Janelle Bird Postdoctoral Research Fellowship. N.M.R. is supported by a NHMRC Investigator and Ideas Grants (GNT2007991 and GNT2001315). A.J.M. is supported by a Queensland Health Advancing Clinical Research Fellowship.

J.S.Y.L., A.M.R., N.M.R., and A.J.M. designed the article. J.S.Y.L. and A.M.R. completed the literature research and drafted the article. J.S.Y.L., A.M.R., N.A.M., M.S.Y.N., N.M.R., and A.J.M. completed edits and review of the article.

Supplemental visual abstract; http://links.lww.com/TP/C648.

Supplemental digital content (SDC) is available for this article. Direct URL citations appear in the printed text, and links to the digital files are provided in the HTML text of this article on the journal's Web site (www.transplantjournal.com).

Correspondence: Andrew J. Mallett, MBBS, FRACP, PhD, Townsville Institute of Health Research and Innovation, Level 2, Townsville University Hospital, Angus Smith Dr, Douglas (Townsville), QLD 4814, Australia. (Andrew.Mallett@health.qld.gov.au).

ISSN: 0041-1337/20/1077-1463

DOI: 10.1097/TP.0000000000004466

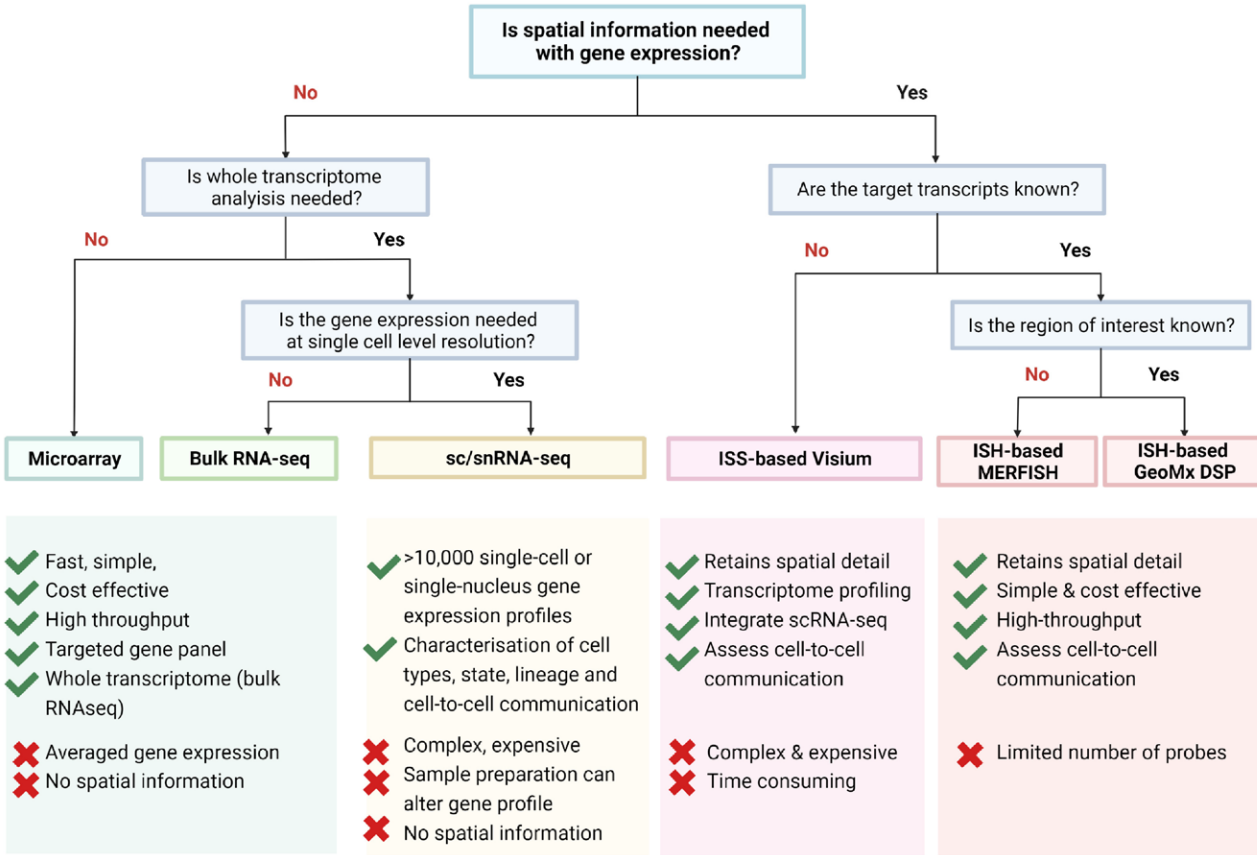

FIGURE 1. Overview of transcriptomic platforms. Available transcriptomics platforms are organized on the basis of a decision hierarchy that can assist transplant researchers to select the right transcriptomics technique for their clinical research question/s. Created using BioRender.com. DSP, Digit Spatial Profiler; ISH, in situ hybridization; ISS, in situ sequencing; MERFISH, multiplexed error-robust fluorescence ISH; sc/snRNA-seq, single-cell/single-nuclei RNA sequencing; ST, spatial transcriptomics.

(including genomics, epigenomics, transcriptomics, proteomics, metabolomics and metagenomics) has allowed researchers to expose the biological processes crucial to immunological matching, transplant rejection, or chronic fibrosis.[2-5] Transcriptomics technologies like microarray, bulk RNA sequencing (RNA-seq), and single-cell or single-nuclei RNA-seq (scRNA-seq or snRNA-seq; Figure 1) have dominated gene profiling research in transplantation over the past 20 y, leading to several large transplantation-based consortia, including the International Genetics and Translational Research in Transplantation Network,[6] Critical Path Institute's Transplant Therapeutics Consortium,[4] Kidney Precision Medicine Project,[7] Genome Canada Transplant Consortium,[8] Banff Molecular Diagnostic Working Group,[9] and Clinical Trials in Organ Transplantation.[10]

Transcriptomics technologies have identified several diagnostic gene panels to improve the detection of kidney, heart, lung, and liver allograft acute rejection when used with traditional histopathology, such as the molecular microscope diagnostics[11-16] (One Lambda), common rejection module,[17] and Banff Human Organ Transplant[9] (B-HOT) panel. In a similar manner, researchers have also identified predictive gene sets for fibrosis and early graft loss in kidney transplants,[18] as well as donor and recipient polygenic risk scores to predict the risk of posttransplant diabetes after liver transplantation.[19] Molecular microscope diagnostics and B-HOT have received the most attention for current and future validation studies. Transcriptomics profiling within archived formalin-fixed and paraffin-embedded (FFPE) tissues have allowed investigators to expand the validation cohorts, including correlation between Banff scores and measurement of the B-HOT gene panel in 326 FFPE kidney transplant biopsies. This panel was able to detect subpathological evidence of rejection (before histopathological features), with peritubular capillary inflammation and donor-specific antibody as primary drivers of antibody-mediated rejection signature.[20] Single-cell transcriptomics have allowed a degree of matching of gene expression to the cell type of origin, although the accuracy of this in human transplant rejection samples is yet to be confirmed.[21,22]

Loss of spatial information is a key limitation with published transcriptomics studies that are high throughput but primarily derived from bulk sample preparations. To retain spatial information, past transcriptomics studies have either used laser capture microdissection (LCM)[23] or serial sections from the same (or sometimes a different) tissue block to select the region of interest (ROI) to infer spatial information. However, the laborious nature of LCM, additional costs, and generally poor spatial information have limited application of LCM-based bulk RNA-seq. Here is where spatial transcriptomics (ST) can provide the critical link between classical gene expression and sc RNA-seq to the underlying cell type(s) and histological structures.

ST methods retain spatial location of the captured transcripts by incorporating either spatial barcode information with in situ sequencing (ISS)–based ST or fluorescently labeled probes with in situ hybridization (ISH)–based ST (Figure 1).

The ISS-ST method captures the genome-wide transcriptome, whereas ISH-ST detects only predefined transcripts. Both methods allow transcripts to be mapped or imaged within their specific spatial location in the tissue section or subcellular structure, respectively, unlike prior methods. The reason spatial information is retained with ISS/ISH-ST techniques is because sample preparation does not require tissue homogenization, cell dissociation, or lysis.[22,24-29] Thus, ST provides the critical link between gene expression and the underlying tissue structures or cell types. This link between gene expression and spatial location within complex tissue sections[30,31] may help discover or clarify key mechanistic processes within solid organ transplantation that can be therapeutically targeted.[32-34] Retention of the spatial context of the transcripts is imperative because complex biological systems, like all solid organs, consist of spatially organized, functional structures, and this is critical to understanding (patho)physiological changes. In this review, we focus on commercially available ST techniques that have allowed transcriptomics to be analyzed within the spatial context of intact tissue sections and thus accounting for complex cellular/structural organization and localized pathologies. We will describe the underlying principles of ST technologies to enable contextualization and highlight opportunities for transplantation-based applications of ST.

SPATIAL TRANSCRIPTOMICS

Both ISS-based and ISH-based ST techniques resolve transcriptome expression within the spatial context of intact tissue. ISS-based ST achieves this by integrating histology with RNA-seq,[24-29,35] whereas ISH-based ST achieves this by expanding on the established fluorescent ISH (FISH) technique. Commercially available ST techniques includes Visium ST-seq (Visium ST, an updated version of the legacy Spatial Transcriptomics) by 10x Genomics, GeoMx Digit Spatial Profiler (DSP) by NanoString (https://nanostring.com), and multiplexed error-robust fluorescence ISH (MERFISH) by Vizgen (https://vizgen.com) (summarized in Figure 2 and Table 1).

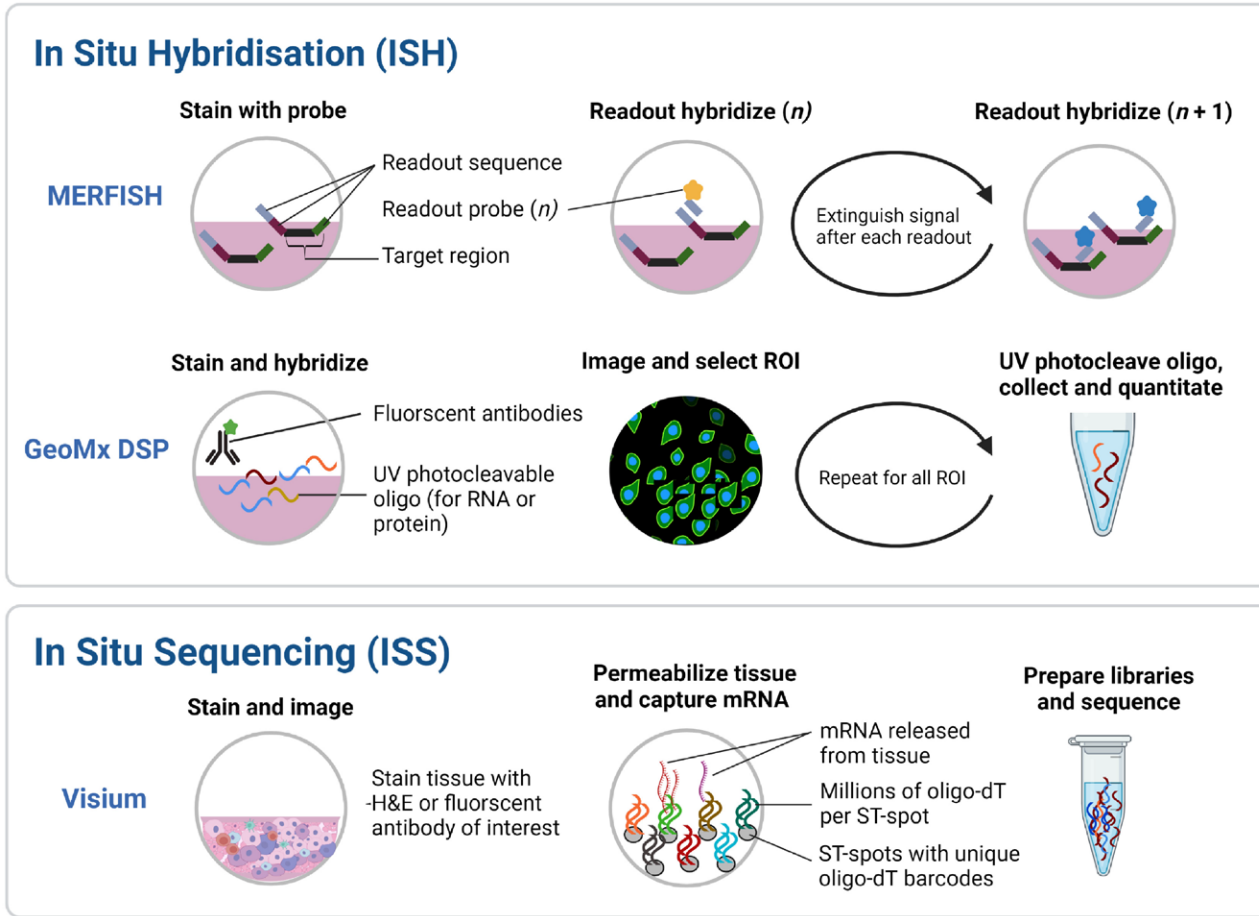

FIGURE 2. Commercially available ST platforms. MERFISH and GeoMx DSP (top panel) are both ISH-based ST techniques that allow fluorescent imaging of targeted genes within the tissue section. Visium (bottom panel) is an ISS-based ST technique that identifies the unbiased gene expression within the tissue section using ST-spots with millions of oligo-dT with unique spatial barcodes. Created using Biorender.com. DSP, Digit Spatial Profiler; H&E, hematoxylin and eosin; ISH, in situ hybridization; ISS, in situ sequencing; MERFISH, multiplexed error-robust fluorescence ISH; oligo-dT, oligonucleotide sequence of repeating deoxythymidines; ROI, region of interest; ST, spatial transcriptomics; UV, ultraviolet.

TABLE 1.

Commercially available ST methods

	Visium	GeoMx DSP	MERFISH
Year commercialized	**2018**	**2019**	**2019**
Company	10x Genomics	NanoString	Vizgen
Reference	https://10xgenomics.com	https://nanostring.com	https://vizgen.com
Staining	Same tissue H&E or immunofluorescence	Same tissue immunofluorescence[a]	Additional tissue needed
Tissue type and capture method	Fresh tissue FFPE tissue Nontargeted Targeted RNA 3′ mRNA[b]	Fresh or FFPE tissue Targeted RNA and protein	Fresh or FFPE tissue Targeted RNA
Capture area and resolution	6.5 × 6.5 mm capture area and 55-µm ST spot–level resolution[c]	ROI ≥200 cells and 32-µm circles resolution[d]	10 mm × 10 mm area and subcellular resolution
Sequencing method	Nontargeted 3′ mRNA sequencing[c]	Targeted dual probes[e]	Targeted fluorescent probes
Sensitivity	>10 000 transcripts for each 55-µm diameter spot	1000 transcripts for each <50-µm ROI	100–1000 genes[f]
Disadvantages	Multiple cells are captured within a single ST-spot	Smaller ROI results in lower sensitivity. ROI must be manually selected	Increase in probes increases cost. Limited to field of view

[a]Limited morphological detail is achieved with fluorescent staining of nuclei, tissue-specific structures (2 fluorescent channels), and cell/protein of interest (third fluorescent channel) to guide the selection of ROI.
[b]Based on the ideal sequencing size of libraries, generated ST libraries will contain ≥254-bp gene insert from the 3′ end, whereas 196bp will comprise 5'–25bp P5 | 10bp Sample Index | 33bp TruSeq Read 1 | 16bp Spatial Barcode | 12bp UMI | 32bp oligo-dT | ≥ 254bp cDNA | 34bp TruSeq Read 2 | 10bp Sample Index | 24bp P7–3′.
[c]Resolution within a 55-µm ST-spot is dependent on the tissue section and the pathology present.
[d]ROI are user-defined and can range from 32- to 400-µm circles. For RNA measurements, the ROI circles must contain 200 cells because RNA targets are not abundant; therefore, smaller ROI circles may introduce selection bias. For protein measurements, the ROI can be increased.
[e]Dual probes system includes both molecular and fluorescent barcodes.
[f]Currently, the maximum number of target probes is 500.
DSP, Digit Spatial Profiler; FFPE, formalin-fixed and paraffin-embedded; H&E, hematoxylin and eosin; MERFISH, multiplexed error-robust fluorescence ISH; oligo-dT, oligonucleotide sequence of repeating deoxythymidines; ROI, region of interest; ST, spatial transcriptomics.

ISH-based ST

For ISH-based ST, there is MERFISH and GeoMx DSP. MERFISH uses encoding probes with a target region complementary to the target transcript and flanking readout sequence that hybridize with fluorescent readout probes. The MERFISH method consists of initial staining with the encoding probe, then sequential rounds of hybridization and imaging of the readout probes across the entire tissue, using custom MERSCOPE. After each round of hybridization and imaging, the fluorescent signals are extinguished and thus, allowing the multiplexing within the MERFISH technique. GeoMx DSP uses fluorescently labeled antibodies and premixed panel ultraviolet photocleavable oligo probes for staining and hybridization with target RNA or protein. After hybridization, the fluorescent antibodies are used to image and select ROIs on a custom GeoMx DSP instrument. These ROIs are then exposed to ultraviolet light to cleave the oligo probes that are collected and quantified on a custom nCounter analysis system or genomic sequencer. In this manner, ISH-based ST has allowed the visualization of tissue niches of interest in complex tissue sections such as brain[36-38] and liver[39] by MERFISH and kidney,[40,41] colon,[42] liver,[43] and lung[44] by GeoMx DSP. Based on the number of probes and size of tissue or ROI, both ISH-based ST techniques are simple, cost-effective, and high-throughput relative to ISS-based ST. However, both ISH-based ST techniques require custom instruments and available probes of known transcripts. Additionally, MERFISH can be limited by sensitivity because of low fluorescent signal and spectral overlap. GeoMx DSP can also be affected by spectral overall and intrinsic limitation to predefined ROI.

ISS-based ST

For ISS-based ST, histology, imaging, and RNA-seq are analyzed sequentially on the same tissue section placed on a glass slide with printed oligonucleotide sequence of repeating deoxythymidines and spatial barcodes within a 55-μm spot, termed ST-spot[34,45,46] (Visium, 10x). Each ST-spot has a unique spatial barcode. As transcriptomes within the tissue section are released by chemical permeabilization, they are captured by the underlying ST-spots and thus receive a spatial barcode. After sequencing, the captured transcriptomes are aligned with the hematoxylin and eosin image of the tissue section to visualize gene expression within the context of the intact tissue.

The current application of ST-seq has allowed the visualization of functional activity in complex tissue sections, including brain, liver, heart, breast, skin, lung, prostate, intestine, and kidney.[47-58] An advantage with commercially available ISS-based ST is that it requires standard histology and molecular laboratory instruments to complete unbiased capture of all transcripts. However, current limitations of the ISS-based ST technique include lateral diffusion of transcripts, poor resolution, and complex bioinformatics analysis. Lateral diffusion of transcript can be mitigated by tissue optimization before commencing an ISS-ST experiment. The poor transcript resolution results because of the capture of mRNA from multiple cells overlying individual ST-spots, which measure 55 μm in diameter. Frequently, the number of cells underlying an individual ST-spot are reported to be 1 to 10 cells. However, the actual number of cells underlying ST-spots depends upon the type of tissue and the pathological processes present within the tissue section. 10x Genomics plan to address this with higher resolution (Visium HD) capture slides to provide a single cell–level ISS-ST platform with smaller and more densely packed ST-spots. Another single-cell ISS-based ST platform currently undergoing commercialization is Slide-seq. The Slide-seq platform uses DNA-barcoded 10-μm beads with probes that can capture, in an unbiased manner, up to 500 transcripts per bead, from fresh frozen tissue sections.[59,60] However, Slide-seq does not incorporate histology and imaging, and therefore, additional adjacent tissue sections are needed to correlate the captured transcriptome with histomorphology. Furthermore, the Slide-seq method requires decoding and identification of the spatial location of the 10-μm beads using sequencing by oligonucleotide ligation and detection.[59-61]

ISS-based ST—Bioinformatics

Bioinformatics workflow components such as quality control, batch correction, normalization, and clustering are similar for both sc/sn RNAseq and ISS-based ST.[25,62,63] However, ISS-based ST has the added complexity of spatial organization with clustering,[48,49,64] annotation, and cell-to-cell communication analysis (Figure 3).[5,10,12,15,17] First, the clustering with ISS-based ST can be mapped back to the tissue section and visually correlated with distinct regions using packages like Seurat,[65] STUtility,[66] Squidpy,[67] and SpatialExperiment.[68] Next, annotation of clusters can be performed on the basis of known structures (ie, glomerulus, tubule, or vessel), regions (ie, cortex versus medulla), or cell types and states (ie, $CD8^+$ T cells with cytotoxic or exhausted states) using known genes for specific regions, structures or cell types and cell states, respectively. Alternatively, this annotation can be completed using label transfer[69,70] or regression-based deconvolution.[70-76] Longo et al[70] provide excellent, in-depth description and discussion of the different annotation strategies. In brief, label transfer uses gene signatures derived from an annotated reference dataset/s to project cell types onto query spatial data sets,[69] resulting in ST-spots being annotated with a nominal cell type based on the dominantly captured transcript.[77] To further predict the single-cell types and states within each ST-spot, there are multiple deconvolution packages.[52,71-75]

However, both label transfer and deconvolution methods require reference data set/s to predict the cell type and/or state within each ST-spot. Generating reference data set/s, which are generally sc/snRNA-seq data sets, can be costly if performed in-house. Publicly available sc/snRNA-seq data sets are a less costly solution. However, if the cell type or state of interest are absent within the reference data set, then integration of additional reference data sets will be needed. The integration of multiple reference data sets needs to be balanced against the introduction of both noise and errors resulting from technical and biological variations between data sets. An analytical alternative to label transfer and deconvolution analysis that does not require a reference data set is BayesSpace[78] that uses the Bayesian statistical method and t-distributed error modeling of the generated spatial clusters to demonstrate reduced noise and clear spatial separation.[78] Once

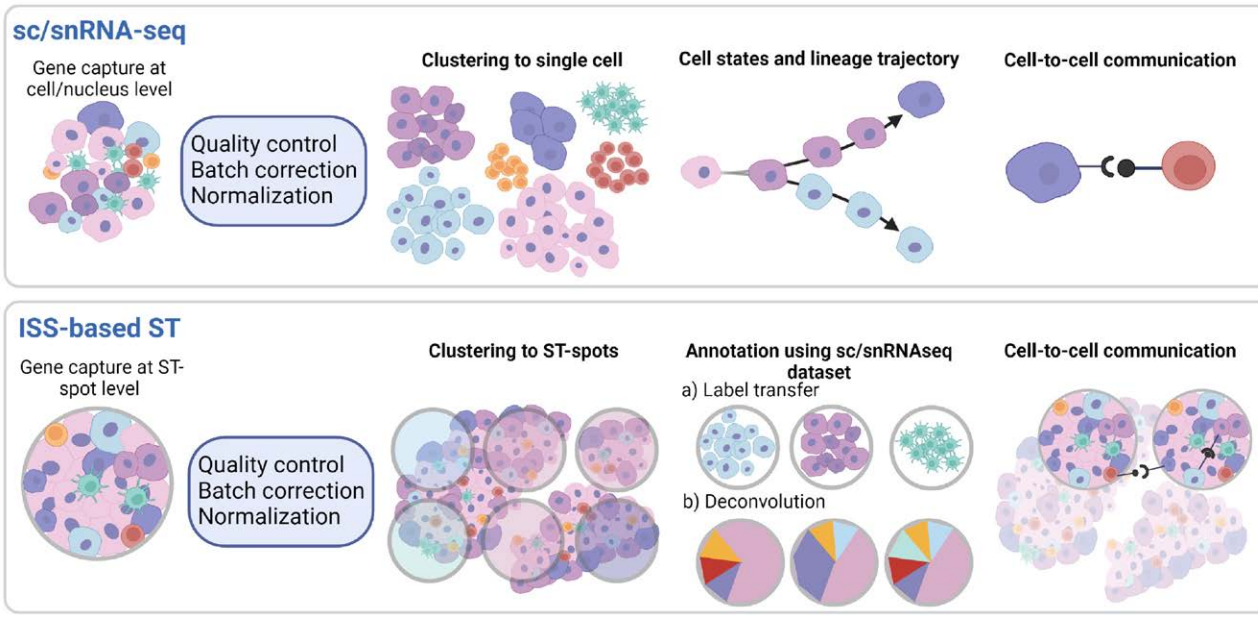

FIGURE 3. Single-cell and ST spot–level gene expression. Bioinformatic analysis of sc/snRNA-seq and ISS-based ST requires similar QC, batch correction, normalization, and clustering. However, with sc/snRNA-seq (top panel), the clustered gene expressions are mapped back to cells (or nuclei), thus, allowing the prediction of cell state, lineage trajectory, and cell-to-cell communication. With ISS-based ST (bottom panel), the clustered gene expressions are mapped back to ST-spots underlying multiple cell types resulting in averaged gene expression. To resolve the averaged gene expression to single-cell level, gene expression within the ST-spots required annotation with label transfer or deconvolution using reference sc/snRNA-seq data sets. The cell-level gene expression within the ST-spots can be mapped back to the tissue section to investigate the spatial organization and colocalization of different cell types and states. Additionally, cell-to-cell communication can be inferred on the basis of the spatial proximity of the cells within and between ST-spots. Created using Biorender.com. ISS, in situ sequencing; QC, quality control; sc/snRNA-seq, single-cell or single-nuclei RNA sequencing; ST, spatial transcriptomics.

ST-spots are annotated then, they can be further characterized into spatial organization, colocalization, and cell–cell communications (within and between ST-spots) using additional analytical approaches.[79] Limitations and risks associated with/without the use and application of reference data sets for annotating ST data sets are best overcome when reliable single-cell or subcellular resolution ST methods are available.

EXPANDING APPLICATION OF ST

A key advantage with Visium, MERFISH, and GeoMx DSP ST techniques is their capacity to complete gene expression profiling in either FFPE or fresh-frozen tissue sections. This ability to use FFPE tissue sections increases sample availability, given that many clinical FFPE specimens are stored after diagnostic testing. However, these samples are especially susceptible to RNA degradation because of delayed and/or poor initial sample handling, fixation, dehydration, and storage.[80,81] Thus, deciding which ST technique to use and when can be difficult. As such, we have provided a simple flowchart (Figure 1) as a guide for selecting an optimal ST technique for the research question/s posed. Given that ST technology has only been commercially available for the past few years, publications using this technique are expected to increase. Most of the studies using spatial technologies are in the areas of organogenesis/embryogenesis, neurological, or cancer research. At the time of this review, the only human transplant-related ST study is by Salem et al.[82] Visium ST-seq experiments have also been performed in a heterotopic heart transplant model, which suggests unique immune cell clusters, but data are limited to a conference abstract.[83] Outside of transplantation, there are several articles that apply spatial technologies to assess the impact of ischemic kidney and cardiac injury, glomerulopathy, as well as diabetes and hypertension on chronic kidney disease (CKD).

Studies in Transplant Rejection Using ST

Salem et al[40] were the first to publish ST data for human kidney chronic T cell–mediated rejection (TCMR) using GeoMx DSP with whole exome sequencing. They selected 2 glomerular and 3 tubulointerstitial ROIs from the TCMR sample and demonstrated tubulointerstitial enrichment of T-cell activation, differentiation, and proliferative pathways for TCMR biopsies compared with control samples. However, the control used in this study was obtained from macroscopically "normal" portions from nephrectomy for renal cell carcinoma, rather than a rejection-free kidney allograft to match for immunological and immunosuppression effects. This difference could impact the differential expression results, even in seemingly "immunologically quiescent" allografts. In addition, using tubulointerstitial ROIs derived from the scarred biopsy (inflammation in areas of interstitial fibrosis and tubular atrophy (i-IFTA) and tubulitis in areas of interstitial fibrosis and tubular atrophy (t-IFTA) = 3 in all 3 ROIs) may explain why the top 100 highly variable genes in the acute rejection biopsy did not correlate with biopsy Banff scores. The supervised selection of 5

individual nonglomerular ROIs for the TCMR kidney demonstrated heterogeneity within the same tissue section, which is both a strength and a weakness. Supervised selection allows assessment of visually distinguishable morphologies, confirms heterogeneity in the underlying transcript expression across space, and highlights the critical nature of obtaining adequate biopsies to avoid sampling error. However, the user-based ROI selection limits the opportunity to apply unbiased clustering to find transcriptomically similar areas in the whole section that could detect novel findings and how well it could "map" back to features identified by histopathologists. There is an opportunity to test how the B-HOT rejection gene panel[9] performs on this sample when the data are accessible.

Future spatial transcriptomic samples of kidney biopsies can help improve biomarker/prediction accuracy by optimizing it for different types of rejection and tissue compartments. With increasing resolution of molecular technologies, it remains to be seen whether this can reliably and accurately predict rejection phenotypes with different clinical trajectories better than the eyes of an experienced pathologist. Combining histology and molecular phenotyping of these biopsies and tracking their long-term outcomes may be useful to guide the immunosuppression burden, particularly patients with subclinical rejection or mixed pathologies such as inflammation associated with BK or cytomegalovirus infections.

Relevant Nontransplant Disease Models Using ST

Smith et al[84] showed that there were distinct glomerular gene expression profiles between human HIV-related versus coronavirus disease 2019–related collapsing glomerulopathy using the NanoString GeoMx DSP platform. A strong interferon-related signature was found in HIV-associated collapsing glomerulopathy but not in coronavirus disease 2019 samples, although there was uncertainty whether this was a result of timing or viral load (positive versus negative polymerase chain reaction) variations at time of biopsy. Comparing collapsing versus "normal" glomeruli had variable numbers of differentially expressed genes within the same biopsy sample (spatial disease heterogeneity). Of interest, they found that paired box gene 8 (*Pax8*), an important transcription factor controlling cell survival and proliferation, was significantly increased in collapsed glomeruli. *Pax8* was detected in visceral epithelial cells and podocytes of the glomerular tuft, compared with "normal" glomeruli derived from the same sample, which was limited to the parietal and tubular epithelium. This approach may be useful for future mechanistic interrogation of glomeruli, peritubular capillaries, and vasculature for transplant-related vasculopathy as well as vascular rejection, particularly for isolated "v" Banff scores.

Kuppe et al[85] recently published a comprehensive study that details the molecular map of abnormal cardiac remodeling after myocardial infarction (MI). This study combined snRNA-seq and single-nuclei assay for transposase-accessible chromatin-seq for chromatin accessibility profiling with ST using Visium ST-seq. Human cardiac samples included control (nontransplanted heart donors), acute MI (ischemic, border and unaffected/remote zones of the LV myocardium), and later stages after MI (fibrotic zones) and were complemented by a murine model of left anterior descending artery occlusion. Not surprisingly, they were able to accurately demarcate ischemic zones, with high levels of immune cell infiltration and proinflammatory signaling linked to the fibroblast-TGF-β–rich cell types and expression in fibrotic zones. By combining snRNA-seq and single-nuclei assay for transposase-accessible chromatin-seq, they were also able to delineate several distinct ventricular cardiomyocyte states, altered metabolic changes in endothelial cells, and myofibroblast differentiation, which all followed distinct spatial patterns depending on normal, injured, and transitioning (border) areas after MI. The vast amount of work and progress in this human MI study[85] provides unique insights into the underlying pathophysiology driving maladaptive remodeling and fibrosis after acute ischemic injury, which may extend to other transplant-related injuries such ischemia-reperfusion injury (IRI) and acute rejection.

Of interest, Kuppe et al[85] performed pseudo-time trajectory analysis to establish a link between scavenger receptor class A member 5 (*Scara5*) rich fibroblasts and differentiated myofibroblasts, which expressed runt-related transcription factor-1 (*Runx1*) and periostin (*Postn*), which are associated with extracellular matrix composition. There was a clear spatial association between myofibroblast markers and secreted phosphoprotein (*Spp1+*) macrophage expression patterns, and their interaction were shown with both receptor–ligand interaction analysis and RNA ISH to support the importance of fibro-myeloid signaling in human hearts. *SPP1+* macrophages were transcriptomically distinct and clustered separately from lymphatic vessel endothelial hyaluronan receptor 1 (*LYVE+*) expressing macrophages. *LYVE1+* macrophages have been detected in vascular smooth muscle cells of human blood vessels,[86] and more recently detected in the medulla of macroscopically normal kidney sections (nephrectomy samples for renal cell carcinoma) using Slide-seqV2.[61] Although their role in renal fibrosis is yet to be established, earlier work demonstrated that depletion of *LYVE+* macrophages led to increased arterial collagen deposition and vascular dysfunction[86] and may be an area of interest for studies into allograft vasculopathy.

Targeted ROIs using GeoMx DSP help improve the resolution limitations of Visium ST-seq, although ST-seq allows analysis of a larger specimen area, which was important for transitional area analysis in the spatial MI study.[85] The larger capture area was exploited by Melo Ferreira et al[87] to show perturbations in metabolic, injury, and prominent neutrophilic pathways in 2 murine acute kidney injury models (IRI, and caecal puncture-ligation) compared with sham-operated mice. The neutrophil signature was localized to the outer stripe (or corticomedullary junction) early after IRI. Deconvolution of spots in this region showed immune-epithelial colocalization (S3-segment proximal tubular cells with either neutrophils or macrophages), and this area also had significantly greater expression of the neutrophil regulator activating transcription factor (*Atf3*). These results were validated using the multiplexed immunofluorescent method, CO-Detection by indEXing.

These studies demonstrate the potential to study allograft injury with spatial detail to unmask important features, which would otherwise be lost with bulk or single-cell (or single-nuclei) dissociation. Currently, the cost

of using these RNA-seq platforms prohibits widespread use or large sample numbers, further limiting its ability to account for variations in age, sex, and transplant vintage in the study design. Dixon et al[88] showed significant differences in the inflammatory response in male versus female mice after IRI, highlighting the need to consider biological sex in study design.[89,90]

CONCLUSION

ST methods will accelerate discovery research in the coming years, and this is particularly likely in the solid organ transplantation field. ST platforms will become more accessible with continued improvements in analytical workflows and cost. Future applications of ST, including further developed or evolved versions of this technology, will benefit both hypothesis generation and targeted transplant research questions. This can potentially aid efforts to use big data to refine transplant rejection phenotypes and scoring[91] by anchoring spatial analysis to histology by machine learning. Spatially resolved analysis of biopsy samples may provide greater sensitivity analysis and interpretation of pathologies, such as acute rejection versus chronic fibrosis areas, to validate current diagnostic/prognostic biomarkers and guide immunosuppression. ST offers a realm of diagnostic and investigative possibilities both prospectively and retrospectively, but it is critical to emphasize that ST must be applied and scrutinized with the same rigor as other methods at our disposal. Despite its enormous potential, data from ST still require careful interpretation of results in context of ≥1 biological or medical questions or hypotheses and cannot replace good experimental design, strong methodology, data quality and sample curation.

REFERENCES

1. Wadström J, Ericzon B-G, Halloran PF, et al. Advancing transplantation: new questions, new possibilities in kidney and liver transplantation. *Transplantation.* 2017;101:S1–S42.
2. Nobakht E, Jagadeesan M, Paul R, et al. Precision medicine in kidney transplantation: just hype or a realistic hope? *Transplant Direct.* 2021;7:e650.
3. Naesens M, Anglicheau D. Precision transplant medicine: biomarkers to the rescue. *J Am Soc Nephrol.* 2018;29:24.
4. Mannon RB, Morris RE, Abecassis M, et al. Use of biomarkers to improve immunosuppressive drug development and outcomes in renal organ transplantation: a meeting report. *Am J Transplant.* 2020;20:1495–1502.
5. Ba R, Geffard E, Douillard V, et al. Surfing the big data wave: omics data challenges in transplantation. *Transplantation.* 2022;106:e114–e125.
6. International Genetics and Translational Research in Transplantation Network (iGeneTRAiN). Design and implementation of the international genetics and translational research in transplantation network. *Transplantation.* 2015;99:2401–2412.
7. de Boer IH, Alpers CE, Azeloglu EU, et al; Kidney Precision Medicine Project. Rationale and design of the kidney precision medicine project. *Kidney Int.* 2021;99:498–510.
8. Sherwood KR, Tran J, Günther OP, et al. Genome Canada precision medicine strategy for structured national implementation of epitope matching in renal transplantation. *Hum Immunol.* 2022;83:264–269.
9. Mengel M, Loupy A, Haas M, et al. Banff 2019 meeting report: molecular diagnostics in solid organ transplantation—Consensus for the Banff Human Organ Transplant (B-HOT) gene panel and open source multicenter validation. *American J Transplant.* 2020;20:2305–2317.
10. Faddoul G, Nadkarni GN, Bridges ND, et al; CTOT-17 Consortium. Analysis of biomarkers within the initial 2 years posttransplant and 5-year kidney transplant outcomes: results from clinical trials in organ transplantation-17. *Transplantation.* 2018;102:673–680.
11. Halloran PF, Pereira AB, Chang J, et al. Microarray diagnosis of antibody-mediated rejection in kidney transplant biopsies: an international prospective study (INTERCOM). *Am J Transplant.* 2013;13:2865–2874.
12. Halloran PF, Potena L, Van Huyen JD, et al. Building a tissue-based molecular diagnostic system in heart transplant rejection: the heart molecular microscope diagnostic (MMDx) system. *J Heart Lung Transplant.* 2017;36:1192–1200.
13. Halloran KM, Parkes MD, Chang J, et al. Molecular assessment of rejection and injury in lung transplant biopsies. *J Heart Lung Transplant.* 2019;38:504–513.
14. Madill-Thomsen K, Abouljoud M, Bhati C, et al. The molecular diagnosis of rejection in liver transplant biopsies: first results of the INTERLIVER study. *Am J Transplant.* 2020;20:2156–2172.
15. Randhawa P. The molecular microscope (MMDX(R)) interpretation of thoracic and abdominal allograft biopsies: putting things in perspective for the clinician. *Clin Transplant.* 2021;35:e14223.
16. Randhawa PS. The molecular microscope diagnostic system (MMDx) in transplantation: a pathologist's perspective. *Am J Transplant.* 2020;20:1965–1966.
17. Khatri P, Roedder S, Kimura N, et al. A common rejection module (CRM) for acute rejection across multiple organs identifies novel therapeutics for organ transplantation. *J Exp Med.* 2013;210:2205–2221.
18. O'Connell PJ, Zhang W, Menon MC, et al. Biopsy transcriptome expression profiling to identify kidney transplants at risk of chronic injury: a multicentre, prospective study. *Lancet.* 2016;388:983–993.
19. Shaked A, Loza B-L, Van Loon E, et al. Donor and recipient polygenic risk scores influence the risk of post-transplant diabetes. *Nat Med.* 2022;28:999–1005.
20. Rosales I, Mahowald G, Tomaszewski K, et al. Banff Human Organ Transplant transcripts correlate with renal allograft pathology and outcome: importance of capillaritis and subpathologic rejection. *J Am Soc Nephrol*. 2022;33:2306–2319.
21. Wu H, Malone AF, Donnelly EL, et al. Single-cell transcriptomics of a human kidney allograft biopsy specimen defines a diverse inflammatory response. *J Am Soc Nephrol.* 2018;29:2069–2080.
22. Malone AF, Humphreys BD. Single-cell transcriptomics and solid organ transplantation. *Transplantation.* 2019;103:1776–1782.
23. Trailin A, Mrazova P, Hruba P, et al. Chronic active antibody-mediated rejection is associated with the upregulation of interstitial but not glomerular transcripts. *Front Immunol.* 2021;12:729558.
24. Lake BB, Codeluppi S, Yung YC, et al. A comparative strategy for single-nucleus and single-cell transcriptomes confirms accuracy in predicted cell-type expression from nuclear RNA. *Sci Rep.* 2017;7:6031.
25. Lake BB, Chen S, Hoshi M, et al. A single-nucleus RNA-sequencing pipeline to decipher the molecular anatomy and pathophysiology of human kidneys. *Nat Commun.* 2019;10:2832.
26. Lacar B, Linker SB, Jaeger BN, et al. Nuclear RNA-seq of single neurons reveals molecular signatures of activation. *Nat Commun.* 2016;7:11022.
27. Wu H, Humphreys BD. The promise of single-cell RNA sequencing for kidney disease investigation. *Kidney Int.* 2017;92:1334–1342.
28. Liao J, Yu Z, Chen Y, et al. Single-cell RNA sequencing of human kidney. *Sci Data.* 2020;7:4.
29. Young MD, Mitchell TJ, Vieira Braga FA, et al. Single-cell transcriptomes from human kidneys reveal the cellular identity of renal tumors. *Science.* 2018;361:594–599.
30. Moses L, Pachter L. Museum of spatial transcriptomics. *Nat Methods.* 2022;19:534–546.
31. Marx V. Method of the year: spatially resolved transcriptomics. *Nat Methods.* 2021;18:9–14.
32. Asp M, Bergenstråhle J, Lundeberg J. Spatially resolved transcriptomes—next generation tools for tissue exploration. *BioEssays.* 2020;42:1900221.
33. Larsson L, Frisén J, Lundeberg J. Spatially resolved transcriptomics adds a new dimension to genomics. *Nat Methods.* 2021;18:15–18.
34. Ståhl PL, Salmén F, Vickovic S, et al. Visualization and analysis of gene expression in tissue sections by spatial transcriptomics. *Science.* 2016;353:78–82.
35. Vickovic S, Ståhl PL, Salmén F, et al. Massive and parallel expression profiling using microarrayed single-cell sequencing. *Nat Commun.* 2016;7:13182.
36. Moffitt JR, Bambah-Mukku D, Eichhorn SW, et al. Molecular, spatial, and functional single-cell profiling of the hypothalamic preoptic region. *Science.* 2018;362:eaau5324.

37. Zhang M, Eichhorn SW, Zingg B, et al. Spatially resolved cell atlas of the mouse primary motor cortex by MERFISH. *Nature.* 2021;598:137–143.
38. Stogsdill JA, Kim K, Binan L, et al. Pyramidal neuron subtype diversity governs microglia states in the neocortex. *Nature.* 2022;608:750–756.
39. Lu Y, Liu M, Yang J, et al. Spatial transcriptome profiling by MERFISH reveals fetal liver hematopoietic stem cell niche architecture. *Cell Discovery.* 2021;7:47.
40. Smith KD, Prince DK, Henriksen KJ, et al. Digital spatial profiling of collapsing glomerulopathy. *Kidney Int.* 2022;101:1017–1026.
41. Ye L, Liu Y, Zhu X, et al. Digital spatial profiling of individual glomeruli from patients with anti-neutrophil cytoplasmic autoantibody-associated glomerulonephritis. *Front Immunol.* 2022;13:831253.
42. Saliba J, Coutaud B, Makhani K, et al. Loss of NFE2L3 protects against inflammation-induced colorectal cancer through modulation of the tumor microenvironment. *Oncogene.* 2022;41:1563–1575.
43. Glennon EKK, Tongogara T, Primavera VI, et al. Elucidating spatially-resolved changes in host signaling during plasmodium liver-stage infection. *Front Cell Infect Microbiol.* 2021;11:804186.
44. Moutafi MK, Molero M, Martinez Morilla S, et al. Spatially resolved proteomic profiling identifies tumor cell CD44 as a biomarker associated with sensitivity to PD-1 axis blockade in advanced non-small-cell lung cancer. *J ImmunoTher Cancer.* 2022;10:e004757.
45. Salmén F, Ståhl PL, Mollbrink A, et al. Barcoded solid-phase RNA capture for spatial transcriptomics profiling in mammalian tissue sections. *Nat Protoc.* 2018;13:2501–2534.
46. Wong K, Navarro JF, Bergenstråhle L, et al. ST spot detector: a web-based application for automatic spot and tissue detection for spatial transcriptomics image datasets. *Bioinformatics.* 2018;34:1966–1968.
47. Sanchez-Ferras O, Pacis A, Sotiropoulou M, et al. A coordinated progression of progenitor cell states initiates urinary tract development. *Nat Commun.* 2021;12:2627.
48. Parigi SM, Larsson L, Das S, et al. The spatial transcriptomic landscape of the healing mouse intestine following damage. *Nat Commun.* 2022;13:828.
49. Joseph DB, Henry GH, Malewska A, et al. 5-Alpha reductase inhibitors induce a prostate luminal to club cell transition in human benign prostatic hyperplasia. *J Pathol.* 2022;256:427–441.
50. Dhainaut M, Rose SA, Akturk G, et al. Spatial CRISPR genomics identifies regulators of the tumor microenvironment. *Cell.* 2022;185:1223–1239.e20.
51. Ma F, Hughes TK, Teles RMB, et al. The cellular architecture of the antimicrobial response network in human leprosy granulomas. *Nat Immunol.* 2021;22:839–850.
52. Wei R, He S, Bai S, et al. Spatial charting of single-cell transcriptomes in tissues. *Nat Biotechnol.* 2022;40:1190–1199.
53. Porritt RA, Zemmour D, Abe M, et al. NLRP3 inflammasome mediates immune-stromal interactions in vasculitis. *Circ Res.* 2021;129:e183–e200.
54. Hildebrandt F, Andersson A, Saarenpää S, et al. Spatial transcriptomics to define transcriptional patterns of zonation and structural components in the mouse liver. *Nat Commun.* 2021;12:7046.
55. Guilliams M, Bonnardel J, Haest B, et al. Spatial proteogenomics reveals distinct and evolutionarily conserved hepatic macrophage niches. *Cell.* 2022;185:379–396.e38.
56. Tavares-Ferreira D, Shiers S, Ray PR, et al. Spatial transcriptomics of dorsal root ganglia identifies molecular signatures of human nociceptors. *Sci Transl Med.* 2022;14:eabj8186.
57. Ratz M, von Berlin L, Larsson L, et al. Clonal relations in the mouse brain revealed by single-cell and spatial transcriptomics. *Nat Neurosci.* 2022;25:285–294.
58. Raghubar AM, Pham, DT, Tan X, et al. Spatially resolved transcriptomes of healthy mammalian kidneys illustrate the molecular complexity and interactions of functional nephron segments. *Front Med* 2022;9:873923.
59. Rodriques SG, Stickels RR, Goeva A, et al. Slide-seq: a scalable technology for measuring genome-wide expression at high spatial resolution. *Science.* 2019;363:1463–1467.
60. Eisenstein M. Companies seek slice of spatial imaging market. *Nat Biotechnol.* 2019;37:490–491.
61. Marshall JL, Noel T, Wang QS, et al. High-resolution slide-seqV2 spatial transcriptomics enables discovery of disease-specific cell neighborhoods and pathways. *iScience.* 2022;25:104097.
62. Melo Ferreira R, Freije BJ, Eadon MT. Deconvolution tactics and normalization in renal spatial transcriptomics. Mini review. *Front Physiol.* 2022;12:812947.
63. Hafemeister C, Satija R. Normalization and variance stabilization of single-cell RNA-seq data using regularized negative binomial regression. *Genome Biol.* 2019;20:296.
64. He Z, Maynard A, Jain A, et al. Lineage recording in human cerebral organoids. *Nat Methods.* 2022;19:90–99.
65. Hao Y, Hao S, Andersen-Nissen E, et al. Integrated analysis of multimodal single-cell data. *Cell.* 2021;184:3573–3587.e29.
66. Bergenstråhle J, Larsson L, Lundeberg J. Seamless integration of image and molecular analysis for spatial transcriptomics workflows. *BMC Genomics.* 2020;21:482.
67. Palla G, Spitzer H, Klein M, et al. Squidpy: a scalable framework for spatial omics analysis. *Nat Methods.* 2022;19:171–178.
68. Righelli D, Weber LM, Crowell HL, et al. SpatialExperiment: infrastructure for spatially resolved transcriptomics data in R using bioconductor. *Bioinformatics.* 2022;38:3128–3131.
69. Stuart T, Butler A, Hoffman P, et al. Comprehensive integration of single-cell data. *Cell.* 2019;177:1888–1902.e21.
70. Longo SK, Guo MG, Ji AL, et al. Integrating single-cell and spatial transcriptomics to elucidate intercellular tissue dynamics. *Nat Rev Genet.* 2021;22:627–644.
71. Cable DM, Murray E, Zou LS, et al. Robust decomposition of cell type mixtures in spatial transcriptomics. *Nat Biotechnol.* 2021;40:517–526.
72. Andersson A, Bergenstråhle J, Asp M, et al. Single-cell and spatial transcriptomics enables probabilistic inference of cell type topography. *Commun Biol.* 2020;3:565.
73. Elosua-Bayes M, Nieto P, Mereu E, et al. SPOTlight: seeded NMF regression to deconvolute spatial transcriptomics spots with single-cell transcriptomes. *Nucleic Acids Res.* 2021;49:e50.
74. Dong R, Yuan G-C. SpatialDWLSaccurate deconvolution of spatial transcriptomic data. *Genome Biol.* 2021;22:145.
75. Song Q, Su J. DSTG: deconvoluting spatial transcriptomics data through graph-based artificial intelligence. *Brief Bioinform.* 2021;22:bbaa414.
76. Sun D, Liu Z, Li T, et al. STRIDE: accurately decomposing and integrating spatial transcriptomics using single-cell RNA sequencing. *Nucleic Acids Res.* 2022;50:e42–e42.
77. Dries R, Chen J, Del Rossi N, et al. Advances in spatial transcriptomic data analysis. *Genome Res.* 2021;31:1706–1718.
78. Zhao E, Stone MR, Ren X, et al. Spatial transcriptomics at subspot resolution with BayesSpace. *Nat Biotechnol.* 2021;39:1375–1384.
79. Armingol E, Officer A, Harismendy O, et al. Deciphering cell–cell interactions and communication from gene expression. *Nat Rev Genet.* 2021;22:71–88.
80. Qiagen. Unlocking your FFPE archive. 2010, Hilden, Germany, www.qiagen.com. Accessed December 2, 2022.
81. Blow N. Tissue preparation: tissue issues. *Nature.* 2007;448:959–963.
82. Salem F, Perin L, Sedrakyan S, et al. The spatially resolved transcriptional profile of acute T cell–mediated rejection in a kidney allograft. *Kidney Int.* 2022;101:131–136.
83. Ainasoja OH, Hurskainen M, Ghimire B, et al. Spatial transcriptomic analysis of acute heart rejection model. *J Heart Lung Transplant.* 2022;41:S301.
84. Smith KD, Prince DK, Henriksen KJ, et al. Digital spatial profiling of collapsing glomerulopathy. *Kidney Int.* 2022;101:1017–1026.
85. Kuppe C, Ramirez Flores RO, Li Z, et al. Spatial multi-omic map of human myocardial infarction. *Nature.* 2022;608:766–777.
86. Lim HY, Lim SY, Tan CK, et al. Hyaluronan receptor LYVE-1-expressing macrophages maintain arterial tone through hyaluronan-mediated regulation of smooth muscle cell collagen. *Immunity.* 2018;49:326–341.e7.
87. Melo Ferreira R, Sabo AR, Winfree S, et al. Integration of spatial and single-cell transcriptomics localizes epithelial cell-immune cross-talk in kidney injury. *JCI Insight.* 2021;6:e147703.
88. Dixon EE, Wu H, Muto Y, et al. Spatially resolved transcriptomic analysis of acute kidney injury in a female murine model. *J Am Soc Nephrol.* 2022;33:279.
89. Aufhauser DD Jr, Wang Z, Murken DR, et al. Improved renal ischemia tolerance in females influences kidney transplantation outcomes. *J Clin Invest.* 2016;126:1968–1977.
90. Wyatt CM, Coates PT, Reeves WB. Of mice and women: do sex-dependent responses to ischemia-reperfusion injury in rodents have implications for delayed graft function in humans? *Kidney Int.* 2016;90:10–13.
91. Vaulet T, Divard G, Thaunat O, et al. Data-driven derivation and validation of novel phenotypes for acute kidney transplant rejection using semi-supervised clustering. *J Am Soc Nephrol.* 2021;32:1084–1096.